Chapter 4

Recent Advances in Heterogeneous Catalytic Hydrogenation of CO_2 to Methane

Zuzeng Qin, Yuwen Zhou, Yuexiu Jiang, Zili Liu and Hongbing Ji

Additional information is available at the end of the chapter

http://dx.doi.org/10.5772/65407

Abstract

With the accelerating industrialization, urbanization process, and continuously upgrading of consumption structures, the CO_2 from combustion of coal, oil, natural gas, and other hydrocarbon fuels is unbelievably increased over the past decade. As an important carbon resource, CO_2 gained more and more attention because of its converting properties to lower hydrocarbon, such as methane, methanol, and formic acid. Among them, CO_2 methanation is considered to be an extremely efficient method due to its high CO_2 conversion and CH_4 selectivity. However, the CO_2 methanation process requires high reaction temperatures (300–400°C), which limits the theoretical yield of methane. Thus, it is desirable to find a new strategy for the efficient conversion of CO_2 to methane at relatively low reaction temperature, and the key issue is using the catalysts in the process. The advances in the noble metal catalysts, Ni-based catalysts, and Co-based catalysts, for catalytic hydrogenation CO_2 to methane are reviewed in this paper, and the effects of the supports and the addition of second metal on CO_2 methanation as well as the reaction mechanisms are focused.

Keywords: catalytic hydrogenation, carbon dioxide, methanation, heterogeneous catalysis, noble metal catalyst, Ni-based catalyst, Co-based catalyst

1. Introduction

Over the past centuries, CO_2 has become the main carbon resource due to the decreases of limited resources such as coal, oil, and natural gas [1]. However, the CO_2 concentration in the atmosphere has consequently increased from ~280 ppm (preindustrial) to ~390 ppm in 2010

at a rate of ca. 1% per year [2], which arguably contributes to the "greenhouse effect," and increases the global temperatures and climate change. CO_2 emissions are still existing threat to humans; it is high time that effective measures should be taken to decrease the emission of CO_2.

Hence, the carbon capture and sequestration (CCS) system is considered to be an efficient method for CO_2 utilization [3, 4]. Nevertheless, the hydrogenation reaction is the most important chemical conversions of CO_2; moreover, which offers a good opportunity for sustainable development in the energy and environmental sectors. Indeed, the reaction process not only reduces the CO_2 amount in the atmosphere but also produces fuels and valuable chemicals [5].

As a promising fuel energy, methane, a simple hydrocarbon, has a wide range of applications in the industry and civil use, which also used to produce some downstream products, such as ethyne, hydrogen, and ammonia [6, 7]; therefore, the strategy of CO_2 methanation is significantly meaningful. Undeniably, the resources of fossil fuels are diminishing and fuel prices have undergone strong fluctuation in recent years. Therefore, developing alternative fuels from nonfossil fuel sources and processes are highly desirable. The products from CO_2 hydrogenation, such as methane, hydrocarbons, methanol, and dimethyl ether, are excellent fuels in internal combustion engines, and are easily stored and transported, but the literature studies showed that the CO_2 conversion to methanol and dimethyl ether is still very low (~20%) and it is difficult to achieve higher conversion of CO_2 [8, 9]. CO_2 methanation is a simple reaction, generating methane under atmospheric pressure with several advantages over other chemicals. Although the conversion was still very low, the CH_4 formation from CO_2 at low temperature has become an important breakthrough in the utilization of CO_2 [10].

CO_2 methanation is a significant catalytic hydrogenation process, as is shown in Eq. (1).

$$CO_2 + 4H_2 \rightarrow CH_4 + 2H_2O, \qquad \Delta H_{298K} = -252.9 KJ \cdot mol^{-1} \tag{1}$$

The methanation of CO_2 has a wide range of applications including the production of syngas and the formation of compressed natural gas [1]. A prototype CO_2 recycling plant to supply clean energy preventing global warming has been built in 1996 using these key materials and has been operating successfully [11]. Without doubt, CO_2 methanation is the key pathway for CO_2 recycling, which requires a catalyst to achieve acceptable rates and selectivities. And extensive studies have been conducted on metal-based catalytic systems in the hydrogenation of CO_2 to methane.

Noble metals (e.g., Ru, Rh, Pd) supported on oxide supports (e.g., TiO_2, Al_2O_3, CeO_2) were the most effective catalysts for CO_2 methanation under relatively mild operating conditions [12–14]; however, the high cost of the catalysts limited their practical applications [15]. Therefore, to obtain a feasible and cost-effective catalytic process, nonnoble metal catalysts (e.g., Ni, Co) were focused by many scholars [16, 17]. This review attempts to present the catalytic reactivity and reaction mechanism over the catalysts, particularly over the heterogeneous catalysts with

http://dx.doi.org/10.5772/65407

an emphasis on the effects of supports and the second metal additives, as well as an overview regarding the challenges and opportunities for future research in the field.

2. Catalysts for CO_2 methanation

2.1. Noble metal catalysts for low-temperature methanation of CO_2

The most widely used catalysts for the CO_2 methanation are noble metals, such as Rh, Ru, and Pd, and Ni-based catalysts. The noble metals are highly active toward CO_2 methanation at lower temperature and more resistant to the carbon formation than other transition metals; however, they are expensive. In particular, the noble metals also used to promote the Ni catalysts to enhance their catalytic activities. The noble metal catalytic systems for the synthesis of methane by CO_2 hydrogenation are summarized in **Table 1**.

Catalyst	Preparation method	*T*/°C	TOF (10^3 s^{-1})	Ref.
0.8 wt% Ru/TiO_2	Polygonal barrel-sputtering	160	8.5	[18]
5 wt% Ru/rutile-TiO_2	Wet-impregnation	160	6.0	[12]
3 wt% Rh/γ-Al_2O_3	Wet-impregnation	200	18.78	[13]
3 wt% Rh/TiO_2	Wet-impregnation	150	22.66	[24]
2 wt% Ru/TiO_2(101)	Hydrothermal	150	4.51	[20]

Table 1. Summarization of activities of CO_2 methanation on noble metal catalysts.

2.1.1. Role of the support on catalyst activity

CO_2 methanation has been studied over a series of supported Ru and Rh catalysts, which were very active for CO_2 hydrogenation [13, 14, 20, 21]. The supports, including Al_2O_3, TiO_2, and CeO_2 for these active metals, have also been investigated. To clarify the influences of the supports on the catalytic behavior of ruthenium, a FT-IR study is used to obtain more insight into the reaction mechanism [21]. Based on the FT-IR spectra of CO and CO_2 adsorbed on the catalysts, the improvement in the CO_2 methanation activity was related to a higher positive polarization of ruthenium on the zeolite, which led to a weaker Ru−CO bond on the H-ZSM-5-supported sample with a corresponding increase of the hydrogen surface coverage, which favors the transformation of the intermediate CO to methane, and which indicated that Ru/ZSM-5 exhibits more CH_4 selectivity than Ru/SiO_2 [21].

The Ru dispersion was significantly influenced by the crystal phase structure of the TiO_2 supports [19]. Rutile-type TiO_2 (r-TiO_2) was a much better support than anatase-TiO_2 (a-TiO_2) in stabilizing of RuO_2 due to the interfacial lattice matching, resulting in a higher reactivity and stability in CO_2 methanation. Owing to the highly dispersed Ru catalyst with a narrow size distribution, r-TiO_2 was a promising support [12]. There was a strong interaction between RuO_2 and r-TiO_2 during the calcination process, which prohibited the aggregation of RuO_2 in

the presence of the Ru–O–Ti bond. As represented in **Figure 1**, upon calcination at 300°C, the Ru/r-TiO_2 exhibited a much higher activity and thermal stability in CO_2 methanation than Ru/a-TiO_2. Moreover, the reaction rate of the Ru/r-TiO_2 was 2.4 times higher than that of the Ru/a-TiO_2, which mainly originated from the different particle sizes of ruthenium [12].

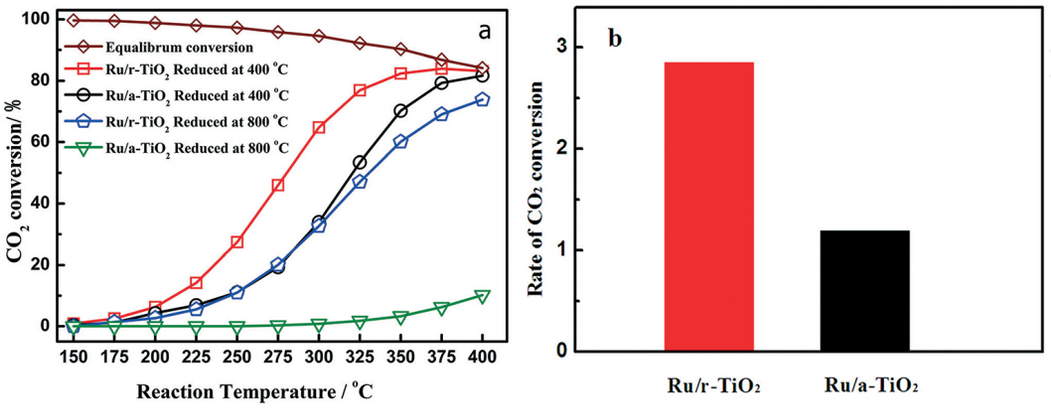

Figure 1. (a) The effects of reaction temperature on the CO_2 conversion over the Ru catalysts and (b) the specific rates of CO_2 conversion calculated at 225°C. The feed gas was 18 vol.% CO_2+ 72 vol.% H_2+ 10 vol.% N_2, and the catalyst was each 0.040 g of Ru/TiO_2 diluted with 0.400 g of SiO_2, the total space velocity was 75,000 mL·g_{cat}^{-1}·h^{-1} [12].

The Ru/TiO_2 catalysts were prepared via a spray reaction (SPR) [20, 22], and the catalytic CO_2 hydrogenation activities of the SPR fine particles were much higher than those of impregnation catalysts [20]. The high activity of the SPR catalysts was attributed to the occurrence of new active sites at the metal-support perimeters without any strong metal-support interaction phenomenon. In addition, highly dispersed Ru nanoparticle-loaded TiO_2 was prepared using a "dry" modification method [18], which markedly enhances the performance of low-temperature methanation, achieving a 100% yield at 160°C. In addition, the methanation reaction over Ru/TiO_2 proceeded at temperatures as low as room temperature with a reaction rate of 0.04 mmol·min^{-1}·g^{-1}.

Although Ru catalysts deposited on different supports, such as alumina, titanium, or silica, have been extensively studied, and the effect of the support on the catalytic properties of small Ru particles in CO_2 hydrogenation has not been fully recognized. Different supports (low and high surface area graphitized carbons, magnesia, alumina and a magnesium-aluminum spinel) were used in CO_2 methanation, and alumina was found to be the most advantageous material [23]. The catalytic properties of very small ruthenium particles are strongly affected by metal-support interactions. In the case of Ru/C, the carbon support partly covers the metal surface, lowering the number of active sites (site blocking). A sequence of the surface-based activities (TOF): Ru/Al_2O_3 > Ru/$MgAl_2O_4$ > Ru/MgO > Ru/C is almost identical to that of electron-deficiencies of the metal, determined by the Lewis acidities of the supports [23].

2.1.2. Effect of metal loading

The most likely effects caused by increasing the loading amount are the growth of the particle size, e.g., the mean particle size of surface Rh species increased with the metal loading amount,

http://dx.doi.org/10.5772/65407

which affected the reactivity [24]. From the study over Rh/γ-Al_2O_3, varying Rh amounts show Rh particle sizes of 3.6–15.4 nm, and a 100% methane selectivity was observed over the entire temperature range and Rh amounts, and the turnover frequency for CH_4 formation depended on the Rh particle size. Larger Rh particles exhibited a catalytic activity of up to four times higher than the smaller particles at 135–150°C, whereas at higher temperatures (200°C) the turnover frequencies are similar for all particle sizes [13].

The Rh loading amount can significantly change the product selectivity of CO_2 hydrogenation over Rh/SiO_2 [25], and the main products transformed from CO_2 to CH_4 with the loading amount of Rh, as shown in **Figure 2**. To the 1 wt% Rh/SiO_2 catalyst, the concentration of surface Rh particles was low, and the Rh species were surrounded by the hydroxyl groups of SiO_2. For the 10 wt% Rh/SiO_2, 5.8 times more surface Rh particles than that of 1 wt% Rh/SiO_2 were found with accordingly less surface hydroxyl groups of SiO_2 existed around Rh particles [25]. In the Ru/Al_2O_3 catalysts with a Ru amount of 0.1–5.0%, the CH_4 selectivity in CO_2 methanation increased with the increase in the Ru loading amount [26]. In the 0.1% Ru/Al_2O_3 catalyst, Ru is mostly present in the atomic dispersion, and the agglomeration of small metal particles (and atoms) in the 3D clusters was observed, indicating a decrease in CH_4 selectivity.

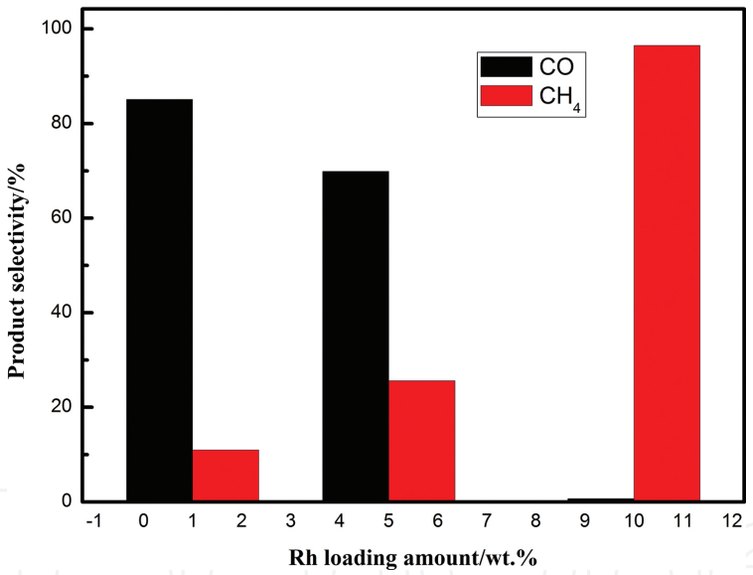

Figure 2. Effect of Rh loading on the distribution of CH_4 and CO [25]. Reaction conditions: temperature = 473 K, pressure = 5 MPa, H_2/CO_2 ratio = 3, flow rate = 100 cm^3 min^{-1}.

2.1.3. Effect of second metal

Actually, when the alkaline salts were added to Ru/Al_2O_3 catalysts, a synergetic effect can be detected, including the electron donation of an alkaline promoter modified the local electron density of the Ru metal, the formation of alkaline chlorides to neutralize the residual chlorine ions, and the removal of the depositional inactive carbon, which was formed on the catalyst surface during CO_2 hydrogenation [22]. Tests of the Ba- and K-containing Rh/Al_2O_3 and the pure Rh/Al_2O_3 in 300–700°C revealed remarkable differences in the cata-

lytic behavior (**Figure 3**). The Ba-containing and especially the pure Rh/Al_2O_3 catalyst showed high selectivity to CH_4 below 500°C with a maximum CH_4 yield of 60% at 400°C; however, at higher temperatures, the CO formation became significant. K-containing Rh/Al_2O_3 converted CO_2 only to CO in 300–700°C and no CH_4 was found. A vastly different adsorption behavior of the Ba- and K-containing catalysts and a significant influence of these additives on the Rh(0)/Rh(I) ratio were revealed [27].

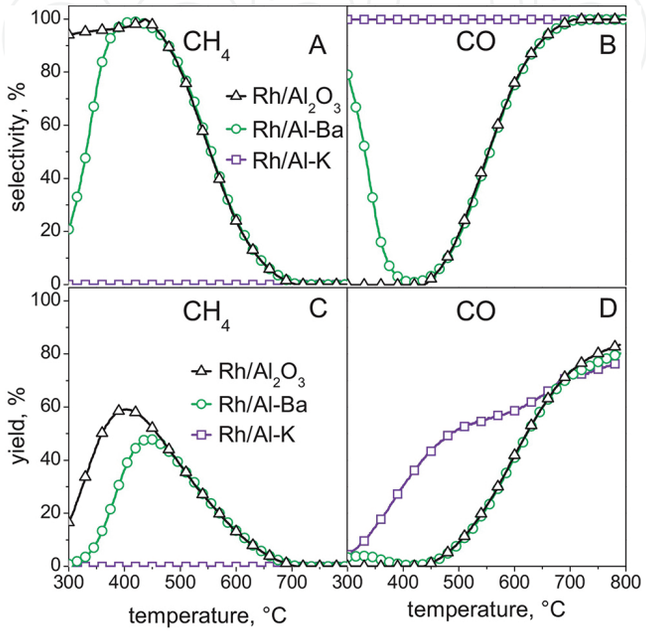

Figure 3. Comparison of selectivity and yield to CH_4 (A and C, respectively) and CO (B and D) is shown as a function of temperature for Ba-containing (circles) and K-containing (squares) Rh/Al_2O_3 catalysts, as well as for pure Rh/Al_2O_3 (triangles) [27].

2.2. Recent advances in Ni-based catalysts

2.2.1. Effect of supports

2.2.1.1. Enhancement of catalytic performance

Choosing a suitable support is mostly according to its properties to activate CO_2 and the interaction between the metal and supports, which is a key parameter for the methanation reaction [28]. The structure and properties of the support do affect the dispersity of active metals and the stability, which enhance the activity of catalysts.

Currently, various materials are used as the supports for nickel catalysts, such as γ-Al_2O_3 [29–31], SiO_2 [32, 33], $Ce_xZr_{1-x}O_2$ [33–36], and TiO_2 [37]. Because the support has a significant influence on the morphology of the active phase, adsorption, and catalytic properties [38], Ni was supported on the mesostructured silica nanoparticles (MSNs), MCM-41, HY zeolite, SiO_2, and γ-Al_2O_3. And the CO_2 methanation activity followed in the order of Ni/MSN > Ni/MCM-41 > Ni/HY > Ni/SiO_2> Ni/γ-Al_2O_3 [32]. The high activity of Ni/MSN is due to the presence of both

intraparticle and interparticle porosities, which led to a high concentration of basic sites. In addition, the defect sites or oxygen vacancies in MSNs were responsible for the formation of surface carbon species, while Ni sites dissociated hydrogen to form atomic hydrogen.

An encouraging result was found in the CO methanation reaction over the zeolite supports, and the same results also found in the Ru/Y and Ru/Al_2O_3 catalysts [39], as well as the supporting Pd on the zeolites, and the catalytic activity on the supporter was in the order of HY > HZSM-5 > NaZSM-5 > NaY > SiO_2 [40]. Similarly, when CO_2 hydrogenation to methane was carried out over nickel species supported on a HNaUSY zeolite, interesting CO_2 conversions and CH_4 selectivities were achieved. CO_2 conversion increased with the Ni content from 2 to 14%, due to the higher amount of Ni^0 species after reduction [41]. Nickel particles were grafted onto SBA-15, and a chemical bond was formed between Ni and Si by O, and no bulk nickel oxides existed in the Ni-grafted SBA-15 [42]. Therefore, the Ni-grafted SBA-15 suited CO_2 methanation, resulting in the higher CO_2 conversion (TOF of 19.4 s^{-1}) and methane selectivity (92%) than a NiO dispersed SBA-15. The status of catalytic systems for the synthesis of methane by CO_2 hydrogenation is summarized in **Table 2**.

Catalyst	Preparation method	T/°C	CO_2 conversion (%)	Methane selectivity (%)	Ref.
20 wt% Ni-Al_2O_3-HT	Coprecipitation	350	82.5	99.5	[31]
20 wt% Ni/Al_2O_3	Impregnation	350	70.8	98.1	[31]
Ni/H−Al_2O_3	Hydrothermal and *in situ* reduction	300	99	99	[43]
15 wt% Ni/TiO_2	Deposition-precipitation	260	96	99	[37]
5 wt% Ni-$Ce_xZr_{1-x}O_2$	Pseudo sol-gel	350	79.7	99.3	[44]
5 wt% Ni-$Ce_xZr_{1-x}O_2$	Hydration process and impregnation	360	71.5	98.5	[48]
5 wt% Ni/MSN	Wet-impregnation	300	64.1	99.9	[32]
5 wt% Ni/MCM-41	Wet-impregnation	300	56.5	98.3	[32]
35 wt% Ni/Fe/Al_2O_3 alumina xerogel	Single step sol-gel	220	63.4	99.5	[45]
10 wt% Ni/MOF-5	Impregnation	320	75.09	100	[46]
14 wt% Ni/USY	Impregnation	400	65.5	94.2	[41]

Table 2. Summary of various Ni catalysts for CO_2 methanation.

2.2.1.2. Nickel dispersion

As a highly active catalyst for CO_2 methanation, a highly uniform dispersed active species over the support is required; therefore, a high specific surface area support is needed. In general, the support usually plays a very important role in the interaction between the Ni and the support. The nickel compounds on different support surfaces result in different "metal-

support effects" [30], which implies that catalysts would exhibit different performance toward activity and selectivity for a given process.

Ni/Al_2O_3 with a high specific surface area showed an excellent controllability on the specific surface area of catalysts with the increase in the Ni amount, and increased the reducibility of the catalyst. However, a further increase in the Ni amount would cause a decrease in CO_2 conversion due to the bigger crystallite size and lower surface area of the catalyst [29, 30]. Indeed, the CO_2 conversion and CH_4 yield are strongly dependent on the Ni amount and the calcination temperature. Compared with the no pretreatment catalysts, the prereduced 16% Ni catalyst obtained 100% CH_4 selectivity with no CO detected [47]. With a higher calcination temperature, the metal nickel is in the form of $NiAl_2O_4$, which is an inactive phase for methanation [47, 48]. The existential state of Ni is usually affected by the support. Cubic metallic Ni particles are found mostly without carbon whiskers, and fast methanation occurs at the expense of the CO intermediate on the corners of nanoparticles interacting with Al_2O_3 [43].

The Ni-based catalyst prepared by coprecipitation is active for CO_2 methanation as well. Coprecipitated Ni/Al_2O_3 catalysts are found to be efficient promoters for CO_2 methanation, and Al_2O_3 is active for CO_2 adsorption [49]. A Ni-Al hydrotalcite-derived catalyst (Ni-Al_2O_3-HT) was prepared by a coprecipitation method with a narrow Ni particle-size distribution and an average particle size of 4.0 nm, a large number of Ni nanoparticles were surrounded by amorphous alumina [31]. As for the Ni amount up to 78 wt%, the average crystalline size of Ni was only 4 nm with a narrow distribution in the range of 3–9 nm. Compared with the 78 wt % Ni/Al_2O_3 catalyst using an impregnation method, the Ni-Al hydrotalcite-derived catalyst exhibited a much higher Ni dispersion than its impregnated counterpart, indicating that Ni-Al hydrotalcite is an ideal precursor for preparation of a well-dispersed Ni catalyst.

Recently, a surface defect-promoted Ni nanocatalyst with a high dispersion and high particle density embedded on a hierarchical Al_2O_3 matrix exhibits excellent activity and stability simultaneously for CO_2 methanation. The abundant surface vacancy clusters serve as the active sites, accounting for the significantly enhanced low-temperature activity of the supported Ni nanoparticles [43]. $Ni/H{-}Al_2O_3(400)$ clearly possesses a significantly enhanced low-temperature activity for CO_2 methanation. The CO_2 conversion exceeded 90% at 265°C and reached the maximal value of 99% at 300°C (**Figure 4A**). The methane production rate increased along with the Ni surface area, indicating a strong correlation between the activity and the Ni surface area. The TOF value as a function of Ni dispersion for the three samples (**Figure 4B**) shows a linear correlation, indicative of a structure sensitive reaction. And the TOF values of the three catalysts toward CO_2 methanation decrease in the following order: $Ni/H{-}Al_2O_3(400) > Ni/H{-}Al_2O_3(500) > Ni/Al_2O_3$ [43].

The different Ni loading amount over the Ni/TiO_2 catalyst strongly affects catalytic CO_2 methanation. When the Ni loading amount was increased to 10 wt%, the selectivity switched to favor the CH_4 formation. Ni nanoparticles (NPs) immobilized on a TiO_2 support were synthesized using a deposition-precipitation method followed by a calcination-reduction process, and the CO_2 conversion and CH_4 selectivity achieved 96 and 99% with a Ni loading of 15 wt% at 260°C [37]. Due to the good dispersion of Ni NPs with large unsaturation facilitates a high exposure of active sites, the formation of surface-dissociated hydrogen and the subse-

http://dx.doi.org/10.5772/65407

quent hydrogenation removal of surface nickel carbonyl species was accelerated, accounting for the resulting enhanced low-temperature catalytic performance [37].

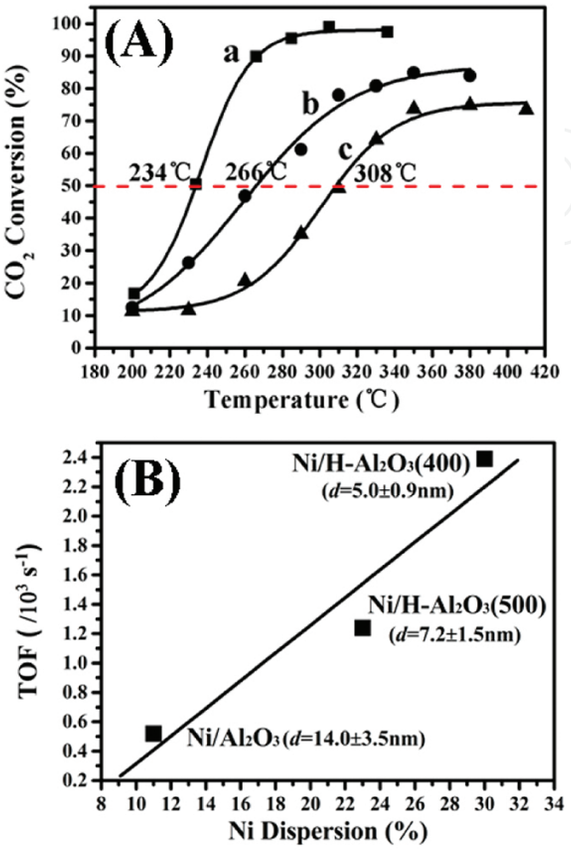

Figure 4. (A) Profiles of CO_2 conversion vs. temperature for CO_2 methanation in the presence of (a) Ni/H–Al_2O_3(400), (b) Ni/H–Al_2O_3(500), and (c) Ni/Al_2O_3 (reacted at 200–410°C and 2400 mL $g_{cat}^{-1}{\cdot}h^{-1}$(WHSV)). (B) The relationship between the TOF value and the Ni dispersion (reacted at 220°C, 9600 mL $g_{cat}^{-1}{\cdot}h^{-1}$(WHSV), and <10% CO_2 conversion) [43].

In the past few years, CeO_2–ZrO_2 solid solution ($Ce_xZr_{1-x}O_2$), an active oxygen material, has been commonly used as a support for automotive three-way catalysts because of its high oxygen storage capacity (OSC), which is important in many reactions [50, 51], and it also used as the support for CO_2 methanation. The Ni-based catalysts on $Ce_xZr_{1-x}O_2$ are greatly efficient in terms of activity and stability, which can be attributed to their high oxygen storage capacities and high Ni dispersion [34–36]. In CO_2 methanation, the Ni^{2+} ion incorporation into the Ni–$Ce_xZr_{1-x}O_2$(Ni–CZ) catalyst significantly enhances the specific catalytic activity of the CZ catalyst [44], and the global catalytic activities of CO_2 methanation on CZ catalysts depended on the surface for available metallic nickel, the composition of the support, and its modification by Ni^{2+} doping. In addition, the $Ce_xZr_{1-x}O_2$ catalyst can be synthesized by a simple hydration process, which achieved the goal of Ce and Ni enriched on the surface [34]. Meanwhile, a new NH_3 reduction method for the preparation of Ni–$Ce_{0.12}Zr_{0.88}O_2$ lead to a higher active metal reducibility, smaller Ni^0 crystallite size, and higher metal dispersion compared to the H_2-

reduction method with 100% CO and 97% CO_2 conversions and ≥ 98% CH_4 selectivity at 250°C [36]. For NH_3-treated samples, the metal dispersion is found to decrease with the increase in Ni amounts due to the formation of bulk Ni particles. However, all H_2-treated samples showed a larger NiO particle size and a lower metal dispersion than the NH_3-treated samples might owing to the H_2-reduced sample exhibits an aggregation of smaller particles and/or metal sintering [36].

Nowadays, metal-organic frameworks (MOFs) have attracted much interest as catalysts and/or supporting materials for active metals or complexes in heterogeneous catalysts [52, 53], e.g., a highly active catalyst Ni/MOF-5 showed unexpected activity at low temperature for CO_2 methanation [46]. For 10Ni/MOF-5, a very high specific surface area of 2961 $m^{-2}{\cdot}g^{-1}$ and a large pore volume of 1.037 $cm^{-3}{\cdot}g^{-1}$ led to a high dispersion of Ni of 41.8%, and the highly uniform dispersion of Ni in the framework of MOF-5 facilitates a high exposure of active sites, resulting the enhancement of the CO_2 conversion to 75.09% and CH_4 selectivity to 100% at 320°C. To further confirm the high dispersion of Ni on the MOF-5 support, the Ni dispersion on MOF-5 and SiO_2 was measured by the H_2 chemisorption. The Ni dispersion on the 10Ni/MOF-5 catalyst was 41.8% as well as that on 10Ni/SiO_2 was 33.7%, as shown in **Figure 5**, which indicated that Ni was more highly dispersed on MOF-5 [46]. In conclusion, the Ni loading amount is dependent on the type of support used, and the Ni loading amount on the support will determine its crystallite size and dispersion on the surface of the support.

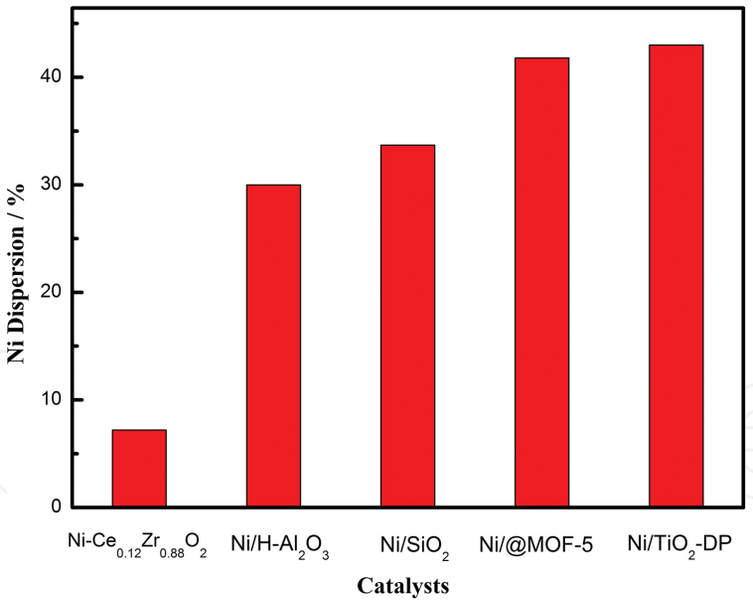

Figure 5. The relation of Ni dispersion and support [36, 37, 43, 46].

2.2.1.3. Catalyst stability

The stability of a catalyst is closely related to the structural destruction, coking, and metal sintering during CO_2 methanation [28, 54]. The long-term catalytic stability and thermal

http://dx.doi.org/10.5772/65407

stability of Ni/H−Al_2O_3 was investigated, the CO_2 conversion decreases slowly in the first 180 h and then remains almost constant with a total decrease of 7% after 252 h. No obvious aggregation or sintering of Ni nanoparticles was observed for the Ni/H−Al_2O_3 catalyst after 252 h upon streaming [43]. Moreover, the control of thermal sintering is critical for maintaining the activity, which requires a stable support and an effective method to prevent particle migration and coalescence [55]. The embedding of Ni nanoparticles onto the Al_2O_3 matrix enhances the metal-support interaction, and prevents the sintering and/or the aggregation of the active nickel species, which shows that the Ni species was embedded in the hierarchical matrix by an *in situ* reduction approach, and the Ni species exhibit a high dispersion degree and high stability, guaranteeing their high activity during the long-term use.

The Ni/MOF-5 catalyst also shows the catalytic activity during 100 h of CO_2 methanation over 10Ni/MOF-5 at 280°C (**Figure 6**). The CO_2 conversion remained above 47.2% and CH_4 selectivity was almost 100% during the 80 h reaction. Obviously, the 10Ni/MOF-5 catalyst was quite stable [46]. However, on $Ce_xZr_{1-x}O_2$ support, the Ce-rich sample (5NiC4Z) showed the better stability from the CO_2 conversions (72.21–62.18%), whereas the CO_2 conversions were 51.63–36.42% and 37.64–23.19% over 5NiCZ and 5NiCZ4, respectively [34]. The higher reducibility of the Ce-rich supported highly-dispersed Ni catalyst was considered to be the important factors to ensure its long-term stability [34].

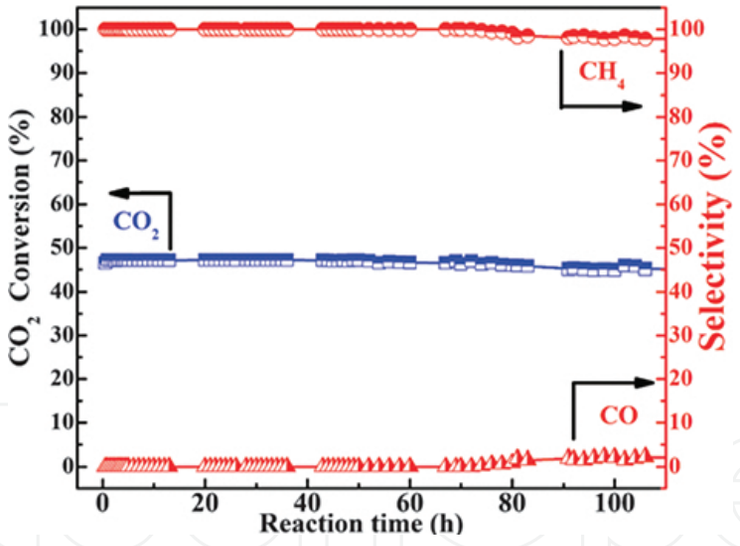

Figure 6. Long-term (100 h) stability tests using the 10Ni/MOF-5 catalyst; reaction conditions: 200 mg catalyst, H_2:CO_2= 4:1, GHSV = 2000 h^{-1}, 1 atm, 280°C [46].

As shown in **Figure 7**, the stability of different Ni supported catalysts was studied, and the rate formation of CH_4 of Ni/MCM-41, Ni/HY, Ni/SiO_2, and Ni/γ-Al_2O_3 catalysts decreases slightly with time on stream increases; however, the rate formation of CH_4 on the Ni/MSN catalyst shows no obvious decrease [32]. In particular, the Ni/MCM-41 shows a minimum percent decrease of the CH_4 formation rate of 3.4%, whereas the Ni/HY, Ni/SiO_2, and Ni/γ-Al_2O_3 is 9.0, 10.6 and 26.6%, respectively. The presence of coke deposition on the active sites is known for the catalyst deactivation; however, no coke content was observed on the Ni/MSN

catalyst from the TGA result and the highest coke content was observed on the Ni/Al_2O_3 catalyst (9.1%), indicating that the Ni/MSN catalyst did not show any sign of deactivation for the methanation reaction up to 200 h of time-on-stream. Therefore, the Ni/MSN catalyst is resistant toward coke formation and presented good stabilities under the reaction conditions [32].

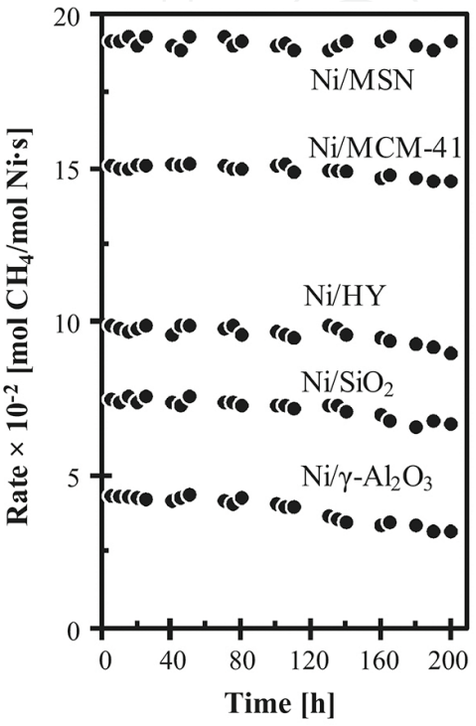

Figure 7. Long-term stability test of Ni catalysts for the CO_2 methanation reaction at a temperature of 573 K, GHSV = 50,000 $mL \cdot g^{-1} \cdot h^{-1}$ and H_2/CO_2= 4:1 [32].

2.2.2. Effect of the second metal

2.2.2.1. Enhancement of catalytic performance

Ni-based catalysts are vulnerable to sintering and coking, which may lead to their deactivation. Hence, many efforts have been made to enhance the catalytic activity, including selection of appropriate supports and addition of catalytic promoters such as Ce, Zr, La, Mg, V, and Co [45, 56, 57]. The most noticeable effect due to the promotion with these metals is a considerable increase both in the CO_2 conversion and CH_4 selectivity under steady conditions.

The catalytic performance of nickel-based catalysts supported on mesoporous nanocrystalline γ-Al_2O_3 promoted with CeO_2, MnO_2, ZrO_2, or La_2O_3 was investigated, and the Ce promoter considerably increases the CO_2 conversion in the methanation reaction (**Table 3**). The addition of the Ce promoter to Ni increased the dissociation and CO_2 hydrogenation, and weakened the C=O bond of CO_2 adsorbed on the Ni active sites. Compared with the unpromoted Ni/Al_2O_3 catalyst, the addition of Ce strengthen the interaction between Ce and Ni, resulting in

http://dx.doi.org/10.5772/65407

better activity of the Ce–Ni/Al_2O_3 catalyst [58]. Doping the Ni-zeolites catalysts with 3–15% of Ce would be much more enhanced the catalytic performance than the unpromoted catalysts [41]. Actually, the presence of CeO_2 after reduction might promote CO_2 activation into CO, the final catalyst properties being due to the synergetic effect between the metal active sites and the promoter.

Catalysts	CO_2 conversion (%)	CH_4 selectivity (%)
20Ni/Al_2O_3	77.2	100
2Ce-20Ni/Al_2O_3	80.3	100
2Mn-20Ni/Al_2O_3	78	100
2La-20Ni/Al_2O_3	75.4	97.6
2Zr-20Ni/Al_2O_3	74.4	99.1

Table 3. Catalytic evaluation of the Ni/Al_2O_3 catalyst with different promoters [56].

Reaction conditions: H_2/CO_2 molar ratio = 3.5, GHSV = 9000 $mL \cdot g_{cat}^{-1} \cdot h^{-1}$ and 350°C.

Some active metals, such as Co, Cu, and Fe, are also used to control the catalytic performance over the supported Ni catalyst, which behave an active aspect as the second metal. Compared with Co and Cu, iron is a suitable second metal for the Ni/ZrO_2 catalyst for low-temperature CO_2 methanation [59], which might be due to its strong electron-donating ability, and Fe^{2+} can promote the reduction of nickel and zirconia. Interestingly, similar results are verified and evaluated the catalytic performance of mesoporous nickel-alumina xerogel catalysts (denote as NiAX) with different second metal (M = Fe, Zr, Ni, Y, and Mg) in a fixed bed reactor (**Table 4**) [45]. However, the oxidized Co is more active toward the methane formation at low temperatures [59, 60], and the Co addition can remarkably change the catalytic performance when active $Ce_xZr_{1-x}O_2$ are used as a support for the Ni catalysts [61]. In addition, a homogeneous alloy of Co and Ni can be formed after H_2 reduction and remain after use for reaction in Co-Ni bimetallic catalysts, which increase the metal dispersion in the catalyst, indicating a certain amount of Co addition can considerably improve the catalytic performance [61, 62].

Catalysts	CO_2 conversion (%)	CH_4 selectivity (%)	CH_4 yield (%)
35Ni5FeAX	63.4	99.5	63.1
35Ni5ZrAX	61.6	99.1	61.0
35Ni5NiAX	61.1	99.2	60.6
35Ni5YAX	58.4	99.5	58.1
35Ni5MgAX	54.2	99.5	53.9

Table 4. Catalytic performance of 35Ni5MAX (M = Fe, Zr, Ni, Y, and Mg) catalysts for methane production from carbon dioxide and hydrogen obtained at 220°C after a 10 h-catalytic reaction [45].

2.2.2.2. Nickel reducibility

In general, the promotion of methanation catalysts with addition of second metals would enhance the nickel reducibility [63, 64]. The improvements in the Co reducibility may occur without any effect on the Co dispersion for the Ni-Ce/USY catalysts [41]. While the effect of promotion with Ce on the Ni reducibility is particularly pronounced with the alumina-supported Ni catalysts [63]. Compared to the unpromoted Ni/Al_2O_3, the lower reduction temperature of NiO in $Ni\text{-}CeO_2/Al_2O_3$ samples implies that addition of CeO_2 decreased the reduction temperature by altering the interaction between Ni and Al_2O_3, and improved the catalyst reducibility [16, 63, 64]. CNTs-supported catalysts exhibited better catalytic performance than the traditional Al_2O_3-supported catalysts [16], which attributed to the outstanding reduction properties of the CNTs-supported catalysts, which provided much more active sites for CO_2 methanation. As shown in H_2-TPR analysis (**Figure 8**), the accession of Ce could effectively promote the reduction of the nickel oxides, the high reduction peak temperature, corresponding to the highly dispersed nickel oxides in intimate contact with the exterior walls of the CNTs, decreased from 480 to 460°C for the 12Ni/CNT and 12Ni4.5Ce/CNT [16], which suggested easily reducible nickel species on the surface of the 12Ni4.5Ce/CNT catalyst, which may due to the interaction change between the metal oxides and CNTs by the addition of cerium.

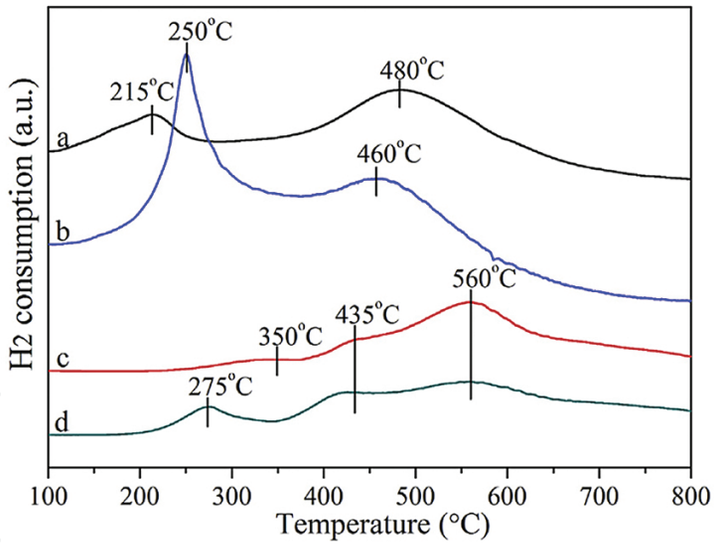

Figure 8. H_2-TPR profiles of the catalysts. (a) 12Ni/CNT, (b) 12Ni4.5Ce/CNT, (c) $12Ni/Al_2O_3$, (d) $12Ni4.5Ce/Al_2O_3$ [16].

Recently, a new kind of $\gamma\text{-}Al_2O_3\text{–}ZrO_2\text{–}TiO_2\text{–}CeO_2$ composite oxide supported Ni-based catalysts was synthesized for CO_2 methanation [65]. The optimal catalytic activity of the composite oxide supported Ni-based catalysts was achieved because of the improvements in the reducibility. According to the H_2-TPR profile for all the catalysts, the high temperature peak (weakly interacted with Al_2O_3, or called Ni rich phase) shifts downward for the composite oxide-supported Ni-based catalysts, suggesting a weaker interaction between NiO and the composite support. Furthermore, the reduction of the Ni rich phase

http://dx.doi.org/10.5772/65407

would benefit the formation of large-sized Ni particles, which are active at low temperatures [66]. Therefore, increasing the fraction of Ni rich phase, i.e., NiO, the active species for the methanation reaction, would result in an increase in the CO_2 conversion at lower temperatures. Moreover, the H_2 consumed amount increased on the composite oxides support, confirming a higher reducibility of NiO on the composite oxides due to the weaker metal-support interaction [65].

2.3. Cobalt-based catalysts for low-temperature methanation of CO_2

Generally, the Co-based Fischer-Tropsch catalysts exhibit a superior catalytic performance with respect to low-temperature CO_2 methanation [17, 67, 68]. A higher CH_4 selectivity was observed in the Fischer-Tropsch synthesis when the Co catalysts were not completely reduced or when the catalysts contain smaller Co_3O_4 particles [67]. When taking the coke oven gas as feed gas and using a nanosized Co_3O_4 catalyst, CO was easily adsorbed onto the smaller nanosized Co_3O_4 surface and react with H_2, and the temperature at which CO completely converted to CH_4 was much lower than that using nanosized Co_3O_4 with large particles [67].

In addition, the Ru-doped Co_3O_4 catalyst with a relatively rough surface shows a lower light-off temperature than that of a Co catalyst [68]. The relatively rough surface morphology of Ru-doped Co_3O_4 probably results from the larger ionic radius of Ru^{3+}, which affects the dissolution-recrystallization process. Therefore, the final surface morphology of nanorods was disrupted with the addition crystalline defects. The correlation between the surface chemistry and the catalytic performances suggests that doping a noble metal to an oxide of an earth-abundant metal followed by reduction could create a chemically stable, cost-effective catalyst with a bimetallic surface, which has an equivalent or much better catalytic performance [68]. Usually, the catalytic activity affected by the catalyst composition and structure, e.g., when used the mesoporous Co/KIT-6 and Co/meso-SiO_2 in CO_2 methanation, the highly ordered bicontinuous mesoporous structure of the Co/KIT-6 catalyst exhibits higher methane selectivity than the Co/meso-SiO_2 catalyst, and the CO_2 conversion exceeds 48.9%, and the methane selectivity can be retained at 100% at 280°C [17].

3. Reaction mechanisms

According to the previous research, the reaction mechanism was difficult to establish mainly because of the different opinions on the intermediate and the methane formation process. Two feasible reaction mechanisms were proposed for CO_2 methanation in the past decades. The first one involves the CO_2 convert to CO prior to methanation, and the subsequent reaction follows the same mechanism as CO methanation [69]. Similar to the mechanism of CO_2 hydrogenation to CH_3OH, someone considered CO was an intermediate [32], and the CO hydrogenation to methane also been focused [70, 71]. The other mechanism involves the direct CO_2 hydrogenation to methane without forming CO as an intermediate [72]. However, the mechanism depends on different catalysis systems, which are still under investigation.

$$H_2 + 2^* \rightarrow 2H^* \quad (2)$$

$$CO_2 + ^* \rightarrow CO_2^* \quad (3)$$

$$CO_2^* + ^* \rightarrow CO^* + O^* \quad (4)$$

$$CO^* + ^* \rightarrow C^* + O^* \quad (5)$$

$$C^* + H^* \rightarrow CH^* \quad (6)$$

$$CH^* + 3H^* \rightarrow CH_4 + ^* \quad (7)$$

$$O^* + H^* \rightarrow OH^* \quad (8)$$

$$OH^* + H^* \rightarrow H_2O^* \rightarrow H_2O + ^* \quad (9)$$

The atomic hydrogen dissociated from Ni sites in the MSN may facilitate the formation of methane, as shown in **Figure 9**. The oxygen vacancies will be formed when H_2 react with the surface oxygen along with the water generation, which activate additional CO_2 to fill the vacancies and produce CO. During the CO_2 methanation reaction, CO was also suggested as the alternative product, which was an intermediate, as shown in Eqs. (2)–(9) [32]. Therefore, the higher CH_4 selectivity can be explained by the enhanced supply of adsorbed hydrogen to the activated adsorbed CO intermediate, which was the rate-determining step [73]. However, some researchers considered that the main mechanism for CO_2 methanation does not require CO as the reaction intermediate [28, 74], which can be explained by the importance of weak basic sites the adsorption of CO_2 [28].

Density functional theory is helpful in understanding the mechanistic aspects of the reactions. Different mechanisms of CO_2 methanation on Ni(111) surfaces were investigated, and the energy barrier of 237.4 kJ mol^{-1} is acquired for the dissociation of CO into C and O species, which support that CO_2 is converted to CO, subsequently to carbon before hydrogenation [75].

As mentioned, the CO_2 adsorption is a crucial step for methanation. Indeed, CO_2 dissociation is the rate-limiting step. CO_2 dissociation over Rh-based catalysts is influenced by the CO coverage on the surface and the strength of the bond Rh−CO, and the hydrogen adsorption at the surface is competed with CO_2 adsorption. Due to the preferential adsorption of CO_2 and the accumulation of CO on the surface, hydrogen coverage on the rhodium catalyst is very

http://dx.doi.org/10.5772/65407

small [76]. However, CO_2 adsorption on the medium basic sites of $Ni/Ce_{0.5}Zr_{0.5}O_2$ results in monodentate carbonates, and monodentate formate derived from monodentate carbonate on medium basic sites, which could be hydrogenated more quickly than bidentate formate derived from hydrogen carbonate. The medium basic sites were proposed to promote the formation of monodentate formate species, thus to enhance the activity [77].

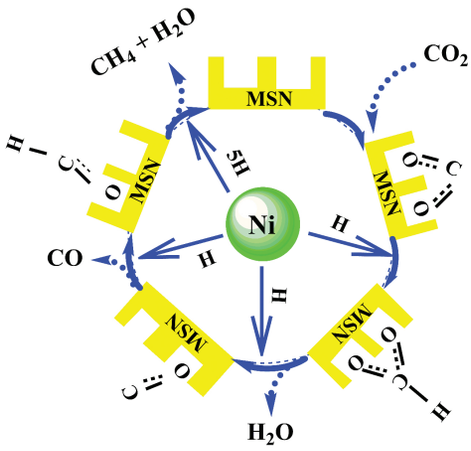

Figure 9. A probable mechanism for Ni/MSN whereby spillover of atomic hydrogen from Ni interacts with C(a) species and sequentially hydrogenates carbon until the product methane desorbs [32].

In addition, at 383 K, a reaction mechanism was proposed for the carbon dioxide methanation reaction on 2% Ru/TiO_2, which investigate the precursor existence for the adsorbed CO and reaction intermediate, and the side-product, formate was also found adsorbing on the support [78], which suggested the surface intermediate corresponding to the adsorbed formate on the metal-support interface, and the measured formate infrared bands are corresponding to the diffused formate species from the interface to the support. A pathway involving hydrogen carbonate is also presented for the formation of the interfacial formate, because the species is formed on the support during the reaction, and the transient response is consistent with the response of a CO precursor. The reaction mechanism that could account for all of these observations is presented in **Figure 10** [78].

To make a better understanding of the adsorption of possible intermediates, the reaction mechanism and factors determining the product selectivity, DFT calculations were considered to be a suitable method to investigate the hydrogenation process of CO_2 and CO on the Ru(0001) surface [79]. For CO_2 hydrogenation, the HCOO intermediate are firstly formed from the adsorbed CO_2 hydrogenation, and subsequently produces an adsorbed CHO and O species. The active C and CH species then undergo stepwise hydrogenation to CH_2, CH_3 and CH_4, or the CHx species, and further transforms to longer carbon chains. From the calculation results, CH_3 hydrogenation is considered to be the rate determining step in the sequence of C hydrogenation on the Ru(0001) surface, and the lowest barrier channel of C–C coupling occurs via the CH + CH reaction [79]. In addition, the study based on DFT calculations on a Ru nanoparticle supported on the TiO_2 catalyst further confirms the stronger electron transfer from the Ru cluster to the $TiO_2(101)$ facet than to $TiO_2(001)$; the Ru species supported on the

(101) plane possesses a relatively lower activation energy for the CO dissociation, resulting in the highly catalytic activity toward CO_2 methanation reaction [80].

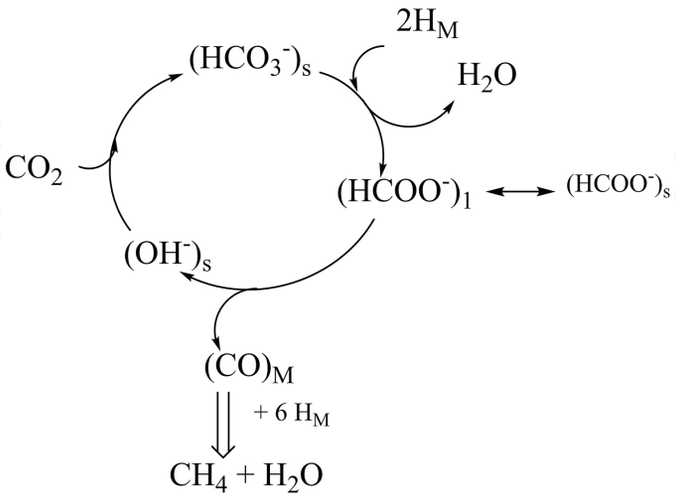

Figure 10. Reaction mechanism of CO_2 methanation [78].

Finally, the detailed mechanism was proposed for CO_2 methanation over metal-based MSNs [81]. As shown in **Figure 11**, CO_2 and H_2 were adsorbed and dissociated on the metal active sites to form CO, O, and H, followed by the migration of these atoms to the MSN surface. Subsequently, the CO dissociated from the active sites interacted with the MSN oxide surfaces to form the carbonyl, including bridged and linear carbonyl, and the H atom in the reaction facilitated the formation of bidentate formate. And the above three species were responsible for the methane formation, among them, the main route for the methane formation was due to the bidentate formate species, and the MSN support served as the sites for carbonyl species, which act as a precursor to methane formation [81].

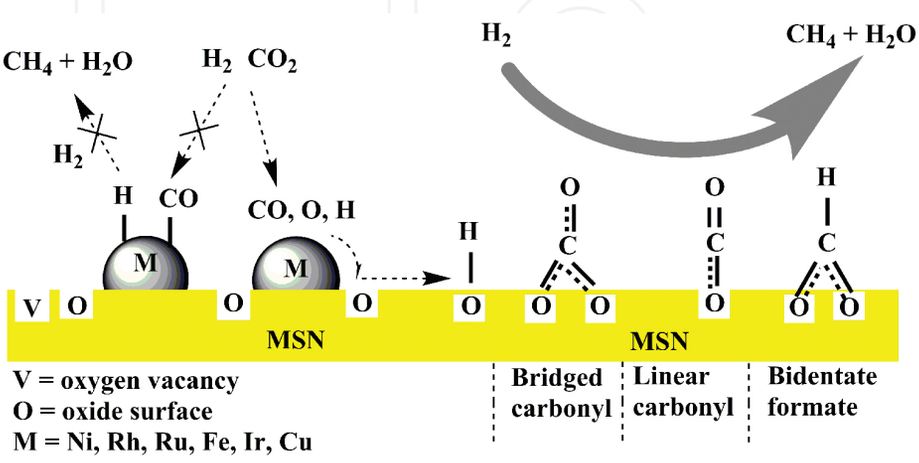

Figure 11. Plausible mechanism of CO_2 methanation on M/MSN [81].

http://dx.doi.org/10.5772/65407

4. Conclusions and perspectives

CO_2 has been promoted to an important carbon resource for conversion and utilization, and CO_2 hydrogenation is a feasible and powerful process, especially for methanation. However, CO_2 is chemically stable and thermodynamically unfavorable. To eliminate the limitations on the conversion and selectivity, various technical directions and specific research approaches on rational design of catalysts and exploration of reaction mechanisms have been presented.

Noble metal catalysts such as Ru, Rh and Pd are efficient for the formation of methane under relatively mild operating conditions, but the high cost as well as their limited availability restricts their practical applications. Therefore, researchers have paid increasing attention on the immobilization of homogenous catalysts to combine the efficient activity with the properties of separation and recyclability. Ni- and Co-based catalysts are, of course, more practical for industrial applications compared to noble metal catalysts. The catalysts with larger surface areas and higher metal dispersion can usually possess higher activity and selectivity, and longer stability in the hydrogenation of CO_2. However, the Ni-based catalysts are more resistless to carbon formation compared with noble metal catalysts. Thus, one strategy has to be proposed for pursuing high-performance catalysts with abilities of low-temperature methanation and resisting carbon formation. In addition, understanding the fundamental mechanisms of CO_2 methanation and explore its relationship with catalyst active site structures using both theoretical calculations (molecular/electronic level modeling) and experimental approaches to tailor new catalyst structures are considerably needed.

Acknowledgements

This work was supported by the National Natural Science Foundation of China (21366004, 21425627) and the Guangxi Natural Science Foundation (2015GXNSFDA139005).

Author details

Zuzeng Qin[1,2*], Yuwen Zhou[1], Yuexiu Jiang[1], Zili Liu[2*] and Hongbing Ji[1,3*]

*Address all correspondence to: qinzuzeng@gmail.com, gzdxlzl@gmail.com and jihb@mail.sysu.edu.cn

1 School of Chemistry and Chemical Engineering, Guangxi University, Nanning, China

2 School of Chemistry and Chemical Engineering, Guangzhou University, Guangzhou, China

3 School of Chemistry and Chemical Engineering, Sun Yat-sen University, Guangzhou, China

References

[1] Wang W, Wang S, Ma X, Gong J. Recent advances in catalytic hydrogenation of carbon dioxide. *Chem Soc Rev*. 2011; 40: 3703–3727. doi: 10.1039/C1CS15008A

[2] Xiaoding X, Moulijn J A. Mitigation of CO_2 by chemical conversion: plausible chemical reactions and promising products. Energy Fuels. 1996; 10: 305–325. doi: 10.1021/ef9501511

[3] Perry R J, O'Brien M J. Amino disiloxanes for CO_2 capture. *Energy Fuels*. 2011; 25: 1906–1918. doi: 10.1021/ef101564h

[4] Wang J, Huang L, Yang R, Zhang Z, Wu J, Gao Y, Wang Q, O'Hare D, Zhong Z. Recent advances in solid sorbents for CO_2 capture and new development trends. *Energy Environ Sci*. 2014; 7: 3478–3518. doi: 10.1039/c4ee01647e

[5] Jessop P G, Joo F, Tai C C. Recent advances in the homogeneous hydrogenation of carbon dioxide. *Coord Chem Rev*. 2004; 248: 2425–2442. doi: 10.1016/j.ccr.2004.05.019

[6] Bai M, Zhang Z, Bai M, Bai X, Gao H. Synthesis of ammonia using CH_4/N_2 plasmas based on micro-gap discharge under environmentally friendly condition. *Plasma Chem Plasma Process*. 2008; 28: 405–414. doi: 10.1007/s11090-008-9132-4

[7] Zeng Y, Wang G. Research and prospects of ethyne from natural gas and its downstream products. *Chem Eng Oil Gas*. 2005; 34: 89–93. doi: 10.1039/b614276a

[8] Bonura G, Cordaro M, Cannilla C, Arena F, Frusteri F. The changing nature of the active site of Cu-Zn-Zr catalysts for the CO_2 hydrogenation reaction to methanol. *Appl Catal B: Environ*. 2014; 152–153: 152–161. doi: 10.1016/j.apcatb.2014.01.035

[9] Liu R-w, Qin Z-z, Ji H-b, Su T-m. Synthesis of dimethyl ether from CO_2 and H_2 using a Cu-Fe-Zr/HZSM-5 catalyst system. *Ind Eng Chem Res*. 2013; 52: 16648–16655. doi: 10.1021/ie401763g

[10] Beuls A, Swalus C, Jacquemin M, Heyen G, Karelovic A, Ruiz P. Methanation of CO_2: Further insight into the mechanism over $Rh/\gamma\text{-}Al_2O_3$ catalyst. *Appl Catal B: Environ*. 2012; 113–114: 2–10. doi: 10.1016/j.apcatb.2011.02.033

[11] Hashimoto K, Habazaki H, Yamasaki M, Meguro S, Sasaki T, Katagiri H, Matsui T, Fujimura K, Izumiya K, Kumagai N, Akiyama E. Advanced materials for global carbon dioxide recycling. *Mater Sci Eng: A*. 2001; 304–306: 88–96. doi: 10.1016/S0921-5093(00)01457-X

[12] Lin Q, Liu X Y, Jiang Y, Wang Y, Huang Y. Crystal phase effects on the structure and performance of ruthenium nanoparticles for CO_2 hydrogenation. *Catal Sci Technol*. 2014; 4: 2058–2063. doi: 10.1039/c4cy00030g

[13] Karelovic A, Ruiz P. CO_2 hydrogenation at low temperature over Rh/gamma-Al_2O_3 catalysts: Effect of the metal particle size on catalytic performances and

reaction mechanism. *Appl Catal B: Environ*. 2012; 113: 237–249. doi: 10.1016/j.apcatb.2011.11.043

[14] Wang F, Li C, Zhang X, Wei M, Evans D G, Duan X. Catalytic behavior of supported Ru nanoparticles on the {100}, {110}, and {111} facet of CeO_2. *J Catal*. 2015; 329: 177–186. doi: 10.1016/j.jcat.2015.05.014

[15] Hetterley R D, Mackey R, Jones J T A, Khimyak Y Z, Fogg A M, Kozhevnikov I V. One-step conversion of acetone to methyl isobutyl ketone over Pd-mixed oxide catalysts prepared from novel layered double hydroxides. *J Catal*. 2008; 258: 250–255. doi: 10.1016/j.jcat.2008.06.017

[16] Wang W, Chu W, Wang N, Yang W, Jiang C. Mesoporous nickel catalyst supported on multi-walled carbon nanotubes for carbon dioxide methanation. *Int J Hydrogen Energy*. 2016; 41: 967–975. doi: 10.1016/j.ijhydene.2015.11.133

[17] Zhou G, Wu T, Xie H, Zheng X. Effects of structure on the carbon dioxide methanation performance of Co-based catalysts. *Int J Hydrogen Energy*. 2013; 38: 10012–10018. doi: 10.1016/j.ijhydene.2013.05.130

[18] Abe T, Tanizawa M, Watanabe K, Taguchi A. CO_2 methanation property of Ru nanoparticle-loaded TiO_2 prepared by a polygonal barrel-sputtering method. *Energy Environ Sci*. 2009; 2: 315–321. doi: 10.1039/b817740f

[19] Kondratenko E V, Amrute A P, Pohl M-M, Steinfeldt N, Mondelli C, Perez-Ramirez J. Superior activity of rutile-supported ruthenium nanoparticles for HCl oxidation. *Catal Sci Technol*. 2013; 3: 2555–2558. doi: 10.1039/c3cy00372h

[20] Li D, Ichikuni N, Shimazu S, Uematsu T. Hydrogenation of CO_2 over sprayed Ru/TiO_2 fine particles and strong metal-support interaction. *Appl Catal A: Gen*. 1999; 180: 227–235. doi: 10.1016/s0926-860x(98)00335-4

[21] Scire S, Crisafulli C, Maggiore R, Minico S, Galvagno S. Influence of the support on CO_2 methanation over Ru catalysts: An FT-IR study. *Catal Lett.* 1998; 51: 41–45. doi: 10.1023/a:1019028816154

[22] Li D, Ichikuni N, Shimazu S, Uematsu T. Catalytic properties of sprayed Ru/Al_2O_3 and promoter effects of alkali metals in CO_2 hydrogenation. *Appl Catal A: Gen*. 1998; 172: 351–358. doi: 10.1016/s0926-860x(98)00139-2

[23] Kowalczyk Z, Stolecki K, Rarog-Pilecka W, Miskiewicz E, Wilczkowska E, Karpiniski Z. Supported ruthenium catalysts for selective methanation of carbon oxides at very low CO_x/H_2 ratios. *Appl Catal A: Gen*. 2008; 342: 35–39. doi: 10.1016/j.apcata.2007.12.040

[24] Hoxha F, van Vegten N, Urakawa A, Krurneich F, Mallat T, Baiker A. Remarkable particle size effect in Rh-catalyzed enantioselective hydrogenations. *J Catal*. 2009; 261: 224–231. doi: 10.1016/j.jcat.2008.12.002

[25] Kusama H, Bando K K, Okabe K, Arakawa H. Effect of metal loading on CO_2 hydrogenation reactivity over Rh/SiO_2 catalysts. *Appl Catal A: Gen*. 2000; 197: 255–268. doi: 10.1016/s0926-860x(99)00486-x

[26] Kwak J H, Kovarik L, Szanyi J. CO_2 reduction on supported Ru/Al_2O_3 catalysts: cluster size dependence of product selectivity. *ACS Catal*. 2013; 3: 2449–2455. doi: 10.1021/cs400381f

[27] Büchel R, Baiker A, Pratsinis S E. Effect of Ba and K addition and controlled spatial deposition of Rh in Rh/Al_2O_3 catalysts for CO_2 hydrogenation. *Appl Catal A*. 2014; 477: 93–101. doi: 10.1016/j.apcata.2014.03.010

[28] Aldana P A U, Ocampo F, Kobl K, Louis B, Thibault-Starzyk F, Daturi M, Bazin P, Thomas S, Roger A C. Catalytic CO_2 valorization into CH_4 on Ni-based ceria-zirconia: Reaction mechanism by operando IR spectroscopy. *Catal Today*. 2013; 215: 201–207. doi: 10.1016/j.cattod.2013.02.019

[29] Rahmani S, Rezaei M, Meshkani F. Preparation of highly active nickel catalysts supported on mesoporous nanocrystalline γ-Al_2O_3 for CO_2 methanation. *J Ind Eng Chem*. 2014; 20: 1346–1352. doi: 10.1016/j.jiec.2013.07.017

[30] Chang F W, Kuo M S, Tsay M T, Hsieh M C. Hydrogenation of CO_2 over nickel catalysts on rice husk ash-alumina prepared by incipient wetness impregnation. *Appl Catal A: Gen*. 2003; 247: 309–320. doi: 10.1016/s0926-860x(03)00181-9

[31] He L, Lin Q, Liu Y, Huang Y. Unique catalysis of Ni-Al hydrotalcite derived catalyst in CO_2 methanation: Cooperative effect between Ni nanoparticles and a basic support. *J Energy Chem*. 2014; 23: 587–592. doi: 10.1016/s2095-4956(14)60144-3

[32] Aziz M A A, Jalil A A, Triwahyono S, Mukti R R, Taufiq-Yap Y H, Sazegar M R. Highly active Ni-promoted mesostructured silica nanoparticles for CO_2 methanation. *Appl Catal B: Environ*. 2014; 147: 359–368. doi: 10.1016/j.apcatb.2013.09.015

[33] Wu H C, Chang Y C, Wu J H, Lin J H, Lin I K, Chen C S. Methanation of CO_2 and reverse water gas shift reactions on Ni/SiO_2 catalysts: The influence of particle size on selectivity and reaction pathway. *Catal Sci Technol*. 2015; 5: 4154–4163. doi: 10.1039/c5cy00667h

[34] Cai W, Zhong Q, Zhao Y. Fractional-hydrolysis-driven formation of non-uniform dopant concentration catalyst nanoparticles of Ni/Ce_xZr_{1-x} O_2 and its catalysis in methanation of CO_2. *Catal Commun*. 2013; 39: 30–34. doi: 10.1016/j.catcom.2013.04.025

[35] Pan Q, Peng J, Sun T, Gao D, Wang S, Wang S. CO_2 methanation on $Ni/Ce_{0.5}Zr_{0.5}O_2$ catalysts for the production of synthetic natural gas. *Fuel Process Technol*. 2014; 123: 166–171. doi: 10.1016/j.fuproc.2014.01.004

[36] Razzaq R, Li C, Amin N, Zhang S, Suzuki K. Co-methanation of carbon oxides over nickel-based $Ce_xZr_{1-x}O_2$ catalysts. *Energy Fuels*. 2013; 27: 6955–6961. doi: 10.1021/ef401049v

[37] Liu J, Li C, Wang F, He S, Chen H, Zhao Y, Wei M, Evans D G, Duan X. Enhanced low-temperature activity of CO_2 methanation over highly-dispersed Ni/TiO_2 catalyst. *Catal Sci Technol*. 2013; 3: 2627–2633. doi: 10.1039/c3cy00355h

[38] Vance C K, Bartholomew C H. Hydrogenation of carbon dioxide on group viii metals. *Appl Catal*. 1983; 7: 169–177. doi: 10.1016/0166-9834(83)80005-0

[39] Elliott D J, Lunsford J H. Kinetics of the methanation reaction over Ru, Ru, Ni, Ru, Cu, and Ni clusters in zeolite Y. *J Catal*. 1979; 57: 11–26. doi: 10.1016/0021-9517(79)90039-3

[40] Saha N C, Wolf E E. CO methanation activity and XPS studies of Pd supported on ZSM-5 and Y-zeolites. *Appl Catal*. 1984; 13: 101–112. doi: 10.1016/S0166-9834(00)83331-X

[41] Graca I, Gonzalez L V, Bacariza M C, Fernandes A, Henriques C, Lopes J M, Ribeiro M F. CO_2 hydrogenation into CH_4 on NiHNaUSY zeolites. *Appl Catal B: Environ*. 2014; 147: 101–110. doi: 10.1016/j.apcatb.2013.08.010

[42] Lu B, Ju Y, Abe T, Kawamoto K. Grafting Ni particles onto SBA-15, and their enhanced performance for CO_2 methanation. *RSC Adv*. 2015; 5: 56444–56454. doi: 10.1039/c5ra07461d

[43] He S, Li C, Chen H, Su D, Zhang B, Cao X, Wang B, Wei M, Evans D G, Duan X. A surface defect-promoted Ni nanocatalyst with simultaneously enhanced activity and stability. *Chem Mater*. 2013; 25: 1040–1046. doi: 10.1021/cm303517z

[44] Ocampo F, Louis B, Kiwi-Minsker L, Roger A-C. Effect of Ce/Zr composition and noble metal promotion on nickel based $Ce_xZr_{1-x}O_2$ catalysts for carbon dioxide methanation. *Appl Catal A: Gen*. 2011; 392: 36–44. doi: 10.1016/j.apcata.2010.10.025

[45] Hwang S, Hong U G, Lee J, Baik J H, Koh D J, Lim H, Song I K. Methanation of carbon dioxide over mesoporous nickel-M-alumina (M = Fe, Zr, Ni, Y, and Mg) xerogel catalysts: Effect of second metal. *Catal Lett*. 2012; 142: 860–868. doi: 10.1007/s10562-012-0842-0

[46] Zhen W, Li B, Lu G, Ma J. Enhancing catalytic activity and stability for CO_2 methanation on Ni@MOF-5 via control of active species dispersion. *Chem Commun*. 2015; 51: 1728–1731. doi: 10.1039/c4cc08733j

[47] Garbarino G, Riani P, Magistri L, Busca G. A study of the methanation of carbon dioxide on Ni/Al_2O_3 catalysts at atmospheric pressure. *Int J Hydrogen Energy*. 2014; 39: 11557–11565. doi: 10.1016/j.ijhydene.2014.05.111

[48] Razzaq R, Zhu H, Jiang L, Muhammad U, Li C, Zhang S. Catalytic methanation of CO and CO_2 in coke oven gas over Ni-Co/ZrO_2-CeO_2. *Ind Eng Chem Res*. 2013; 52: 2247–2256. doi: 10.1021/ie301399z

[49] Aksoylu A E, Akin A N, Önsan Z İ, Trimm D L. Structure/activity relationships in coprecipitated nickel-alumina catalysts using CO_2 adsorption and methanation. *Appl Catal A: Gen*. 1996; 145: 185–193. doi: 10.1016/0926-860X(96)00143-3

[50] Wang Q, Li G, Zhao B, Shen M, Zhou R. The effect of La doping on the structure of $Ce_{0.2}Zr_{0.8}O_2$ and the catalytic performance of its supported Pd-only three-way catalyst. *Appl Catal B: Environ*. 2010; 101: 150–159. doi: 10.1016/j.apcatb.2010.09.026

[51] Zhao M, Shen M, Wang J. Effect of surface area and bulk structure on oxygen storage capacity of $Ce_{0.67}Zr_{0.33}O_2$. *J Catal*. 2007; 248: 258–267. doi: 10.1016/j.jcat.2007.03.005

[52] Mueller M, Hermes S, Kaehler K, van den Berg M W E, Muhler M, Fischer R A. Loading of MOF-5 with Cu and ZnO nanoparticles by gas-phase infiltration with organometallic precursors: Properties of Cu/ZnO@MOF-5 as catalyst for methanol synthesis. *Chem Mater*. 2008; 20: 4576–4587. doi: 10.1021/cm703339h

[53] Hermes S, Schroter M K, Schmid R, Khodeir L, Muhler M, Tissler A, Fischer R W, Fischer R A. Metal@MOF: Loading of highly porous coordination polymers host lattices by metal organic chemical vapor deposition. *Angew Chem-Int Ed*. 2005; 44: 6237–6241. doi: 10.1002/anie.200462515

[54] Razzaq R, Li C, Usman M, Suzuki K, Zhang S. A highly active and stable Co_4N/gamma-Al_2O_3 catalyst for CO and CO_2 methanation to produce synthetic natural gas (SNG). *Chem Eng J*. 2015; 262: 1090–1098. doi: 10.1016/j.cej.2014.10.073

[55] Rostrup-Nielsen J R, Pedersen K, Sehested J. High temperature methanation: Sintering and structure sensitivity. *Appl Catal A: Gen*. 2007; 330: 134–138. doi: 10.1016/j.apcata.2007.07.015

[56] Rahmani S, Rezaei M, Meshkani F. Preparation of promoted nickel catalysts supported on mesoporous nanocrystalline gamma alumina for carbon dioxide methanation reaction. *J Ind Eng Chem*. 2014; 20: 4176–4182. doi: 10.1016/j.jiec.2014.01.017

[57] Zhi G, Guo X, Wang Y, Jin G, Guo X. Effect of La_2O_3 modification on the catalytic performance of Ni/SiC for methanation of carbon dioxide. *Catal Commun*. 2011; 16: 56–59. doi: 10.1016/j.catcom.2011.08.037

[58] Enrique Daza C, Gamba O A, Hernandez Y, Centeno M A, Mondragon F, Moreno S, Molina R. High-stable mesoporous Ni-Ce/clay catalysts for syngas production. *Catal Lett*. 2011; 141: 1037–1046. doi: 10.1007/s10562-011-0579-1

[59] Ren J, Qin X, Yang J-Z, Qin Z-F, Guo H-L, Lin J-Y, Li Z. Methanation of carbon dioxide over Ni-M/ZrO_2 (M = Fe, Co, Cu) catalysts: Effect of addition of a second metal. *Fuel Process Technol*. 2015; 137: 204–211. doi: 10.1016/j.fuproc.2015.04.022

[60] Khodakov A Y, Griboval-Constant A, Bechara R, Zholobenko V L. Pore size effects in Fischer Tropsch synthesis over cobalt-supported mesoporous silicas. *J Catal*. 2002; 206: 230–241. doi: 10.1006/jcat.2001.3496

[61] Zhu H, Razzaq R, Li C, Muhmmad Y, Zhang S. Catalytic methanation of carbon dioxide by active oxygen material $Ce_xZr_{1-x}O_2$ supported Ni-Co bimetallic nanocatalysts. *AICHE J*. 2013; 59: 2567–2576. doi: 10.1002/aic.14026

[62] Guo M, Lu G. The regulating effects of cobalt addition on the catalytic properties of silica-supported Ni-Co bimetallic catalysts for CO_2 methanation. *React Kinetic Mechan Catal*. 2014; 113: 101–113. doi: 10.1007/s11144-014-0732-0

[63] Liu H, Zou X, Wang X, Lu X, Ding W. Effect of CeO_2 addition on Ni/Al_2O_3 catalysts for methanation of carbon dioxide with hydrogen. *J Nat Gas Chem*. 2012; 21: 703–707. doi: 10.1016/s1003-9953(11)60422-2

[64] Zhou L, Wang Q, Ma L, Chen J, Ma J, Zi Z. CeO_2 Promoted mesoporous Ni/gamma-Al_2O_3 catalyst and its reaction conditions for CO_2 methanation. *Catal Lett*. 2015; 145: 612–619. doi: 10.1007/s10562-014-1426-y

[65] Abate S, Mebrahtu C, Giglio E, Deorsola F, Bensaid S, Perathoner S, Pirone R, Centi G. Catalytic performance of gamma-Al_2O_3-ZrO_2-TiO_2-CeO_2 composite oxide supported Ni-based catalysts for CO_2 methanation. *Ind Eng Chem Res*. 2016; 55: 4451–4460. doi: 10.1021/acs.iecr.6b00134

[66] Zhang J, Xu H Y, Jin X L, Ge Q J, Li W Z. Characterizations and activities of the nano-sized Ni/Al_2O_3 and Ni/La-Al_2O_3 catalysts for NH_3 decomposition. *Appl Catal A: Gen*. 2005; 290: 87–96. doi: 10.1016/j.apcata.2005.05.020

[67] Zhu H, Razzaq R, Jiang L, Li C. Low-temperature methanation of CO in coke oven gas using single nanosized Co_3O_4 catalysts. *Catal Commun*. 2012; 23: 43–47. doi: 10.1016/j.catcom.2012.02.029

[68] Zhu Y, Zhang S, Ye Y, Zhang X, Wang L, Zhu W, Cheng F, Tao F. Catalytic conversion of carbon dioxide to methane on ruthenium–cobalt bimetallic nanocatalysts and correlation between surface chemistry of catalysts under reaction conditions and catalytic performances. *ACS Catal*. 2012; 2: 2403–2408. doi: 10.1021/cs3005242

[69] Lapidus A L, Gaidai N A, Nekrasov N V, Tishkova L A, Agafonov Y A, Myshenkova T N. The mechanism of carbon dioxide hydrogenation on copper and nickel catalysts. *Petrol Chem*. 2007; 47: 75–82. doi: 10.1134/s0965544107020028

[70] Fujita S I, Takezawa N. Difference in the selectivity of CO and CO_2 methanation reactions. *Chem Eng J*. 1997; 68: 63–68. doi: 10.1016/s1385-8947(97)00074-0

[71] Kraselcuk R, Isli A I, Aksoylu A E, Onsan Z I. CO hydrogenation over bimetallic nickel-vanadium catalysts. *Appl Catal A: Gen*. 2000; 192: 263–271. doi: 10.1016/S0926-860X(99)00409-3

[72] Schild C, Wokaun A, Baiker A. On the mechanism of CO and CO_2 hydrogenation reactions on zirconia-supported catalysts: A diffuse reflectance FTIR study: Part II. Surface species on copper/zirconia catalysts: Implications for methanoi synthesis selectivity. *J Mol Catal*. 1990; 63: 243–254. doi: 10.1016/0304-5102(90)85147-A

[73] Roldan L, Marco Y, Garcia-Bordeje E. Function of the support and metal loading on catalytic carbon dioxide reduction using ruthenium nanoparticles supported on carbon nanofibers. *Chemcatchem*. 2015; 7: 1347–1356. doi: 10.1002/cctc.201500016

[74] Upham D C, Derk A R, Sharma S, Metiu H, McFarland E W. CO_2 methanation by Ru-doped ceria: The role of the oxidation state of the surface. *Catal Sci Technol*. 2015; 5: 1783–1791. doi: 10.1039/c4cy01106f

[75] Ren J, Guo H, Yang J, Qin Z, Lin J, Li Z. Insights into the mechanisms of CO_2 methanation on Ni(111) surfaces by density functional theory. *Appl Surf Sci*. 2015; 351: 504–516. doi: 10.1016/j.apsusc.2015.05.173

[76] Swalus C, Jacquemin M, Poleunis C, Bertrand P, Ruiz P. CO_2 methanation on Rh/γ-Al_2O_3 catalyst at low temperature: "In situ" supply of hydrogen by Ni/activated carbon catalyst. *Appl Catal B: Environ*. 2012; 125: 41–50. doi: 10.1016/j.apcatb.2012.05.019

[77] Pan Q, Peng J, Sun T, Wang S, Wang S. Insight into the reaction route of CO_2 methanation: Promotion effect of medium basic sites. *Catal Commun*. 2014; 45: 74–78. doi: 10.1016/j.catcom.2013.10.034

[78] Marwood M, Doepper R, Renken A. In-situ surface and gas phase analysis for kinetic studies under transient conditions: The catalytic hydrogenation of CO_2. *Appl Catal A: Gen*. 1997; 151: 223–246. doi: 10.1016/S0926-860X(96)00267-0

[79] Zhang S-T, Yan H, Wei M, Evans D G, Duan X. Hydrogenation mechanism of carbon dioxide and carbon monoxide on Ru(0001) surface: A density functional theory study. *RSC Adv*. 2014; 4: 30241–30249. doi: 10.1039/c4ra01655f

[80] Wang F, Zhang S, Li C, Liu J, He S, Zhao Y, Yan H, Wei M, Evans D G, Duan X. Catalytic behavior of supported Ru nanoparticles on the (101) and (001) facets of anatase TiO_2. *RSC Adv.* 2014; 4: 10834–10840. doi: 10.1039/c3ra47076h

[81] Aziz M A A, Jalil A A, Triwahyono S, Sidika S M. Methanation of carbon dioxide on metal-promoted mesostructured silica nanoparticles. *Appl Catal A: Gen*. 2014; 486: 115–122. doi: 10.1016/j.apcata.2014.08.022